

Localization of a dipolar Bose-Einstein condensate in a bichromatic optical lattice

P. Muruganandam^{1,2}‡, R. Kishor Kumar², and S. K. Adhikari¹ §

¹Instituto de Física Teórica, UNESP - Universidade Estadual Paulista, 01.140-070 São Paulo, São Paulo, Brazil

²School of Physics, Bharathidasan University, Palkalaiperur Campus, Tiruchirappalli 620024, Tamilnadu, India

Abstract. By numerical simulation and variational analysis of the Gross-Pitaevskii equation we study the localization, with an exponential tail, of a dipolar Bose-Einstein condensate (DBEC) of ^{52}Cr atoms in a three-dimensional bichromatic optical-lattice (OL) generated by two monochromatic OL of incommensurate wavelengths along three orthogonal directions. For a fixed dipole-dipole interaction, a localized state of a small number of atoms (~ 1000) could be obtained when the short-range interaction is not too attractive or not too repulsive. A phase diagram showing the region of stability of a DBEC with short-range interaction and dipole-dipole interaction is given.

PACS numbers: 67.85.Hj,03.75.Lm,03.75.Nt

‡ murganand@gmail.com

§ adhikari@ift.unesp.br; URL: www.ift.unesp.br/users/adhikari

1. Introduction

The localization of a non-interacting wave form in a disordered potential, predicted by Anderson [1], has been the topic of vigorous research in different areas. Localization has been observed experimentally in diverse contexts [2] including Bose-Einstein condensates (BEC) [3, 4]. Billy *et al.* [3] demonstrated the localization of a cigar-shaped interacting ^{87}Rb BEC released into a one-dimensional (1D) waveguide with controlled disorder created by a laser speckle. Roati *et al.* [4] observed the localization of a non-interacting ^{39}K BEC in a bichromatic quasi-periodic optical-lattice (OL) potential created by superposing of two standing-wave polarized laser beams with incommensurate wavelengths. The non-interacting BEC was created [4] by tuning the atomic scattering length a to zero near a Feshbach resonance [5]. The disorder in a quasi-periodic OL potential is deterministic, in contrast to the complete disorder in a optical speckle potential. The localization in such a quasi-periodic potential is a special case of Anderson localization in a fully disordered potential and is well described by the Aubry-André model [6]. Such a localization is often termed Aubry-André localization. However, these two mechanisms of localization are distinct. While Anderson localization of wave functions with exponential tails is a pure quantum effect, the Aubry-André localization may occur in a classical phase space [7]. The localization of a BEC in a disordered potential has been the subject matter of various theoretical [8, 9, 10, 11, 12] and experimental [2, 3, 4] studies.

In the presence of strong disorder one has strong Anderson localization [3, 4], where the localized state could be quite similar to a localized state of Gaussian shape in an infinite potential or a potential of very high barriers. Then the quantum state cannot escape the strong barriers of the disordered potential. However, the more interesting case of localization is in the presence of a weak disorder when the system is localized due to the quasi-periodic (disordered) nature of the potential [3, 4] and not due to the strength of the lattice. The localization takes place due to cancellation of waves coming after multiple scattering from many barriers of the random potential. When this happens the localized state acquires a pronounced exponential tail.

The usual dilute BEC with negligible dipole moment interacting via short-range interaction is described by the mean-field Gross-Pitaevskii (GP) equation. More recently, it has been possible [13] to obtain a BEC of ^{52}Cr atoms with large dipole moment leading to a long-range dipole-dipole (dipolar) interaction superposed on the usual short-range interaction, which can be varied using a Feshbach resonance [5]. This allows to study the dipolar BEC (DBEC) of ^{52}Cr atoms with variable short-range interaction [13]. Because of the anisotropic dipolar interaction, the DBEC possesses many distinct features [13, 14, 15, 16, 17], which are under active investigation by different research groups [18, 19]. For example, the stability of a DBEC depends not only on the value of the scattering length, but also strongly on the geometry of the trapping potential [13, 14, 15]. A pancake-shaped trapping potential give a repulsive mean field of dipolar interaction and thus the dipolar condensate is more stable. In

contrast, a cigar-shaped trapping potential yields an attractive mean-field of dipolar interaction and hence leading to a dipolar collapse [13, 20, 21, 22, 23]. Peculiarities in the collective low energy shape oscillations of DBEC have been studied by Yi and You [21]. Analogue of roton-maxon instability and the appearance of roton minimum in Bogoliubov spectrum [24, 25] and angular collapse of DBEC [26] have been studied. Numerical studies on the stability shows certain unusual structure of the Hartree ground state of dipolar condensate in an anisotropic trap [15, 16].

After the experiment [4] on the localization of a 1D BEC in a quasi-periodic trap, a natural extension of this phenomenon would be to achieve localization in two and three dimensions (3D) [27, 12], both for a BEC and a DBEC. The theoretical description of a dilute weakly-interacting DBEC can be formulated by including a dipolar interaction term in the GP equation maintaining the formal simplicity, nevertheless, increasing vastly the numerical complexity. Using the numerical and variational solutions of the GP equation, we study the localization of a BEC and a DBEC in 3D, in the presence of bichromatic OL potentials along orthogonal directions. Although the localized states have an exponential tail in a weak quasi-periodic potential, the central part of such localized states, responsible for the major contribution to the total density, may have a Gaussian distribution. In the present paper we shall consider such localized states with an exponential tail and a Gaussian central part, which can also be studied by the variational approximation. The variational approximation provides an analytical understanding of the localization and also yields interesting result when the numerical procedure is difficult to implement. Such a variational Gaussian approximation has successfully been applied to the localization of a BEC without dipolar interaction in one [10], two and three dimensions [12] in a bichromatic OL potential as well as a speckle potential [11] in one dimension.

Due to the angle dependence of the long-range dipolar interaction, the localization of a DBEC is more interesting than a BEC with only a short-range interaction. The dipolar interaction is weak in the spherically-symmetric shape, is attractive in the cigar shape (aligned dipoles arranged linearly attract each other) and repulsive in the pancake shape (aligned dipoles arranged side-by-side repel each other) [19]. Because of this, the trap configuration plays an essential role in the localization of a DBEC. The controllable short-range interaction together with the exotic dipolar interaction makes the DBEC an attractive system for experimental localization in a bichromatic OL potential and a challenging system for theoretical investigation allowing to study the interplay between the dipolar interaction and the short-range interaction in dipolar atoms.

The cigar- and pancake-shaped localized DBEC are obtained by considering bichromatic OL potentials of different strengths along the orthogonal directions. A localized DBEC, without short-range interaction, can be achieved in a bichromatic OL trap for a small number of atoms by tuning [13] the atomic scattering length to zero near a Feshbach resonance [5]. For a cigar-shaped DBEC, without short-range interaction, as the number of atoms increases it becomes highly attractive and suffers from collapse instability. In the presence of a repulsive short-range interaction, the effect

of the attractive dipolar interaction in the cigar shape can be compensated leading to a localized DBEC for a small number of atoms; delocalization may take place due to excess of repulsion for a large number of atoms. For a pancake-shaped DBEC, the dipolar interaction is repulsive and a localized DBEC is obtained for a small number of atoms. For a large number of atoms excess of repulsion should lead to delocalization. From a variational analysis of the localization of a DBEC, a phase diagram illustrating its stability for different short-range interaction, number of atoms, and the geometry of the bichromatic OL is given. To obtain localization, the short-range interaction should be small. As in 1D [9, 10, 28], a large repulsive short-range interaction destroys the localization and the localized state escapes to infinity in all cases. A large attractive short-range interaction leads to collapse instability and destroys the localization.

In Sec. II we present a brief account of the modified GP equation with the bichromatic OL potential in the presence of a dipolar interaction together with a Gaussian variational analysis. In Sec. III we present numerical and variational studies of localization of a dipolar dipolar interaction in the presence and absence of a short-range interaction. In Sec. IV we present a brief summary of the present investigation.

2. Analytical Formulation

We shall study the localization of the DBEC of N atoms, each of mass m , using the following mean-field GP equation with bichromatic OL potential $V(\mathbf{r})$: [13]

$$\frac{m}{\hbar^2}\mu\phi(\mathbf{r}) = \left[-\frac{1}{2}\nabla^2 + V(\mathbf{r}) + 4\pi aN|\phi(\mathbf{r})|^2 + \int U_{dd}(\mathbf{r}-\mathbf{r}')|\phi(\mathbf{r}')|^2 d\mathbf{r}' \right] \phi(\mathbf{r}), \quad (1)$$

with

$$U_{dd}(\mathbf{r}) = 3Na_{dd}(1 - 3\cos^2\theta)/r^3, \quad (2)$$

and

$$V(\mathbf{r}) = \sum_{l=1}^2 A_l[\nu_\rho\{\sin^2(k_l x) + \sin^2(k_l y)\} + \nu_z \sin^2(k_l z)], \quad (3)$$

where $\phi(\mathbf{r})$ is the DBEC wave function of normalization $\int \phi(\mathbf{r})^2 d\mathbf{r} = 1$, μ is the chemical potential, a the atomic scattering length, θ is the angle between \mathbf{r} and the direction of polarization, here taken along the z axis, $A_l = k_l^2 s_l/2$, λ_l 's are the wave lengths, $k_l = 2\pi/\lambda_l$ are the wave numbers, and s_l are the strengths of the OL potentials. The parameters ν_ρ and ν_z control the relative strengths of the OL's in different directions and can be varied to achieve the pancake- ($\nu_z > 1, \nu_\rho = 1$) and cigar-shaped ($\nu_\rho > 1, \nu_z = 1$) DBEC. The constant $a_{dd} = \mu_0 \bar{\mu}^2 m / (12\pi \hbar^2)$ in the dipolar interaction U_{dd} is a length characterizing the strength of dipolar interaction and its experimental value for ^{52}Cr atoms is $15a_0$ [13], with a_0 the Bohr radius, $\bar{\mu}$ the (magnetic) dipole moment of a single atom, and μ_0 the permeability of free space.

The GP equation (1) can be solved variationally by minimizing the energy

functional [13]

$$\frac{m}{\hbar^2}E[\phi] = \int \left[\frac{1}{2} |\nabla\phi|^2 + \sum_{j=1}^d V(\mathbf{r})\phi^2 + 2\pi a N \phi^4 + \frac{\phi^2}{2} \int U_{dd}(\mathbf{r}-\mathbf{r}') |\phi(\mathbf{r}')|^2 d\mathbf{r}' \right] d\mathbf{r} \quad (4)$$

with the following Gaussian ansatz for $\phi(\mathbf{r})$ [29]:

$$\phi(\mathbf{r}) = \left(\frac{\pi^{-3/2}}{w_\rho^2 w_z} \right)^{1/2} \exp \left(-\frac{\rho^2}{2w_\rho^2} - \frac{z^2}{2w_z^2} \right), \quad (5)$$

where w_ρ is the width in the radial direction ρ and w_z is the width in the axial direction z . We have assumed circular symmetry in the $x-y$ plane. Equations (4) and (5) lead to [29]

$$\begin{aligned} \frac{m}{\hbar^2}E &= \frac{1}{4} \left[\frac{2}{w_\rho^2} + \frac{1}{w_z^2} \right] + \frac{N}{\sqrt{2\pi}} \frac{1}{w_\rho^2 w_z} [a - a_{dd}f(\kappa)] \\ &\quad + \frac{1}{2} \sum_{l=1}^2 A_l [2\nu_\rho + \nu_z - 2\nu_\rho \mathcal{E}_{\rho,l} - \nu_z \mathcal{E}_{z,l}], \end{aligned} \quad (6)$$

$$f(\kappa) = \frac{1 + 2\kappa^2}{1 - \kappa^2} - \frac{3\kappa^2 \operatorname{atanh}\sqrt{1 - \kappa^2}}{(1 - \kappa^2)^{3/2}}, \quad \kappa \equiv \frac{w_\rho}{w_z}, \quad (7)$$

where $\mathcal{E}_{\rho,l} = \exp(-w_\rho^2 k_l^2)$, $\mathcal{E}_{z,l} = \exp(-w_z^2 k_l^2)$. For a stationary state the energy mE/\hbar^2 should have a minimum as a function of w_ρ and w_z : $\partial E/\partial w_\rho = \partial E/\partial w_z = 0$, together with the condition

$$\left(\frac{\partial^2 E}{\partial w_\rho \partial w_z} \right)^2 - \frac{\partial^2 E}{\partial w_\rho^2} \frac{\partial^2 E}{\partial w_z^2} < 0. \quad (8)$$

The minima conditions $\partial E/\partial w_\rho = \partial E/\partial w_z = 0$ become in explicit notation

$$2\nu_\rho w_\rho^4 \sum_{l=1}^2 A_l k_l^2 \mathcal{E}_{\rho,l} - \frac{N}{\sqrt{2\pi} w_z} [2a - a_{dd}g(\kappa)] = 1, \quad (9)$$

$$2\nu_z w_z^4 \sum_{l=1}^2 A_l k_l^2 \mathcal{E}_{z,l} - \frac{2N w_z}{\sqrt{2\pi} w_\rho^2} [a - a_{dd}h(\kappa)] = 1, \quad (10)$$

where

$$g(\kappa) = \frac{2 - 7\kappa^2 - 4\kappa^4}{(1 - \kappa^2)^2} + \frac{9\kappa^4 \operatorname{atanh}\sqrt{1 - \kappa^2}}{(1 - \kappa^2)^{5/2}}, \quad (11)$$

$$h(\kappa) = \frac{1 + 10\kappa^2 - 2\kappa^4}{(1 - \kappa^2)^2} - \frac{9\kappa^2 \operatorname{atanh}\sqrt{1 - \kappa^2}}{(1 - \kappa^2)^{5/2}}. \quad (12)$$

The solution of (9) – (12) determine the widths w_z and w_ρ . For a certain set of parameters, localization is possible if there is a minimum of the energy. Hence from (6) and (9) – (12) we can determine if a BEC or DBEC would be localized or not.

3. Numerical Study

We perform a full 3D numerical simulation in Cartesian x, y, z variables using imaginary- and real-time propagation with Crank-Nicolson discretization [30] employing small space

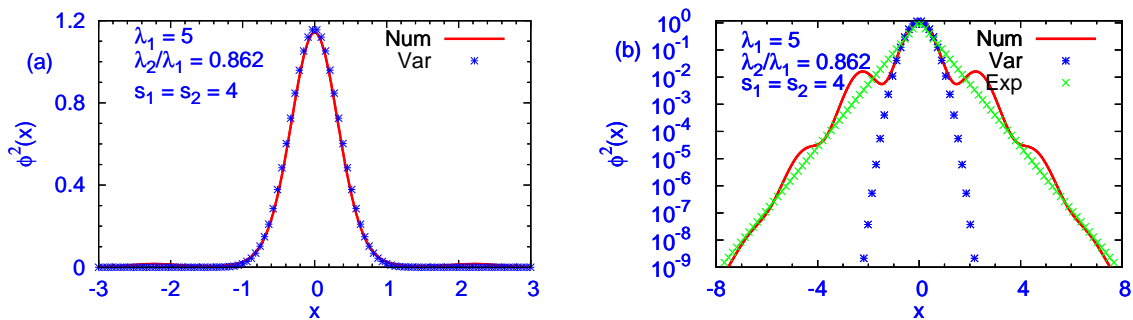


Figure 1. (Color online) (a) Normalized numerical (Num) and variational (Var) densities $\phi^2(x)$ of (13) versus x for the 1D localized state with bichromatic OL wave lengths $\lambda_1 = 5$, $\lambda_2 = 0.862\lambda_1$, and strengths $s_1 = s_2 = 4$. (b) The same densities together with the exponential fit $\phi^2(x) = \exp[-2\text{abs}(x)/l_{\text{loc}}]/(0.4865\sqrt{\pi})$, $l_{\text{loc}} = 0.75$ on a log scale.

(~ 0.025) and time (~ 0.0001) steps necessary for obtaining converged results. For this purpose we use the FORTRAN programs provided in [31] after transforming (1) into a time-dependent form by replacing $m\mu/\hbar^2$ by $i\partial/\partial t$, where t is time. The dipolar interaction term is evaluated by the usual fast Fourier transformation technique [14]. The imaginary- and real-time propagation lead essentially to the same localized states. This not only assures the correctness of the calculational scheme, but also guarantees that the localized states are stationary and not a result of dynamical self-trapping [32]. (The imaginary-time propagation can only find the stationary localized states and cannot obtain the dynamical self-trapped states.) The stability of the localized state was tested by real-time propagation allowing small perturbations of potential or interaction parameters. (In the absence of the dipolar interaction, the localized states have been demonstrated explicitly to be stable in one [10] and two [12] dimensions.) The accuracy of the numerical simulation was tested by varying the size of space and time steps and the total number of space and time steps.

To compare the numerical results with variational analysis, we only consider localized states mostly occupying a single site of the bichromatic OL. Throughout this study the strength parameters of the two components of the bichromatic OL are taken as $s_1 = s_2 = 4$ and the corresponding wave lengths are taken as $\lambda_1 = 5 \mu\text{m}$, $\lambda_2 = 0.862\lambda_1$. The relative strength of the radial and axial bichromatic optical lattice are varied by adjusting the parameters ν_ρ and ν_z in Eq. (3). To demonstrate that with these sets of parameters we are in the limit of localization with an exponential tail in a weak potential, we solve the 1D linear Schrödinger equation in dimensionless variables [31]

$$-\frac{1}{2}\phi''(x) + \sum_{l=1}^2 \frac{2\pi^2 s_l}{\lambda_l^2} \sin^2\left(\frac{2\pi}{\lambda_l}x\right) \phi(x) = \mathcal{E}\phi(x), \quad (13)$$

with the above sets of parameter, where the prime denotes x -derivative and \mathcal{E} denotes energy. In the limit of zero nonlinearity ($a = 0$) and zero dipolar interaction ($a_{dd} = 0$), (1) decouples into three equations like (13). In figure 1 (a) and (b) we plot the density

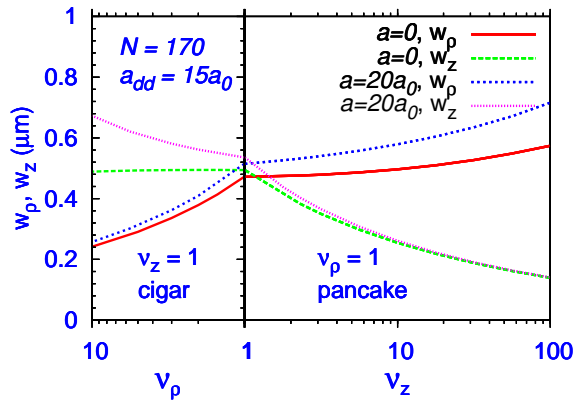


Figure 2. (Color online) Variational widths w_ρ and w_z of the DBEC versus bichromatic OL relative strength parameters ν_ρ and ν_z [viz. Eq. (3)] for 170 ^{52}Cr atoms for scattering length $a = 0$ and $20a_0$.

$\phi^2(x)$ of (13) versus x in linear and log scales together with its Gaussian variational counterpart $\phi^2(x) = \exp(-x^2/w^2)/(\pi^{1/2}w)$, with $w = 0.4865$ the variational width, and the exponential fit $\phi^2(x) = \exp[-\text{abs}(x)/l_{\text{loc}}]/(0.4865\pi^{1/2})$, with $l_{\text{loc}} = 0.75$ the localization length [3] providing a measure of the exponential tail. For strong localization with strong bichromatic potential $l_{\text{loc}} \rightarrow 0$ and the localized state has a pure Gaussian tail. However, when $l_{\text{loc}} > x_{\text{rms}}$ with x_{rms} the root mean square size, the exponential tail is pronounced and the limit of localization in a weak quasi-periodic potential is attained [3, 4]. In the present example, $x_{\text{rms}} = 0.53$ and $l_{\text{loc}} = 0.75$, and hence we are in the limit of localization in a weak potential. This is clear from figure 1 (b), where the central part of the localized state is fitted to the variational Gaussian solution, whereas the large- x parts are fitted to an exponential function with a large localization length over about nine orders of magnitude. In figure 1 (b), one can identify several minor peaks in successive wells of the bichromatic OL potential. The state of figure 1 is localized by the weak bichromatic lattice and if we substantially reduce the strength of the potential, no localized state will emerge. In the experiments of Refs. [3, 4] and in some other studies on localization [9] in a weak potential, localized states with a pronounced undulating tail over many wells of the localization potential were considered. However, a weak limit of localization with an exponential tail can also be achieved in the absence of a pronounced undulating tail, as we have shown here. In this paper we shall be considering localization in the presence of a pronounced Gaussian peak and a weak undulating tail as can be seen from figure 1 (b). The existence of a pronounced Gaussian peak will be turned to a good advantage in predicting accurate analytical variational results for the localized state and for an analytical understanding of the localization. We shall also consider the localization in the presence of short-range interaction and dipolar interaction. The inclusion of a repulsive short-range interaction will in general destroy localization by increasing the localization length and thus creating a more pronounced exponential tail

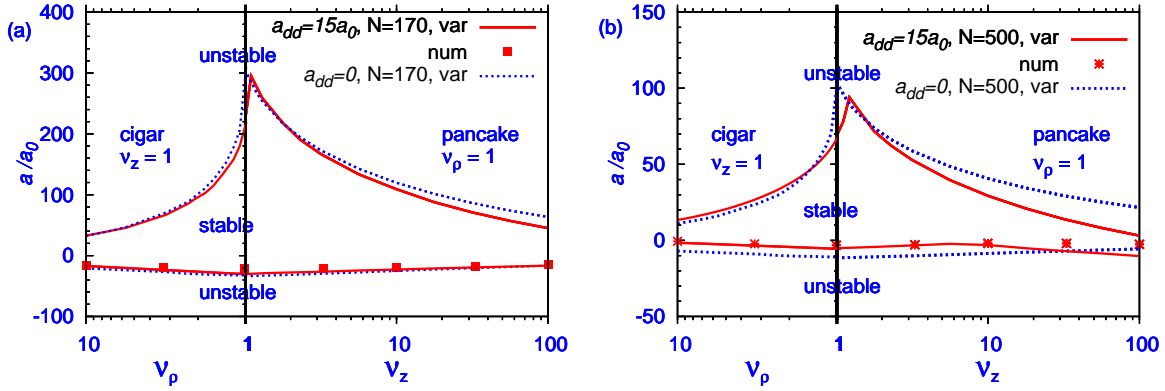


Figure 3. (Color online) Stability region in the a/a_0 versus ν_ρ and ν_z (relative strengths of the bichromatic OL in radial and axial directions) phase plots for (a) 170 and (b) 500 atoms for $a_{dd} = 15a_0$ (^{52}Cr atoms) and $a_{dd} = 0$ variational - var (lines), numerical - num (points). Localization is possible between the upper and lower lines of the same data set.

[9]. The inclusion of the dipolar interaction will have an effect on localization, which we shall study here, and such inclusion should not destroy the exponential tail of localization as illustrated in figure 1 (b).

A variational analysis is useful for a qualitative understanding of the problem and we present the same before considering a numerical solution of (1). In figure 2 we plot the variational widths w_ρ and w_z for a DBEC of 170 ^{52}Cr atoms in the cigar and pancake shapes. This figure shows the evolution of the widths from the pancake to cigar shapes while the radial width w_ρ reduces and the axial width w_z increases as expected. For $a = 0$, the axial width w_z does not increase with the increase of ν_ρ , as in the cigar shape the dipolar interaction becomes attractive and does not permit the increase of w_z .

Next we study, using (6), the set of values of the parameters for which the energy can have a minimum and allows a stable localized DBEC. The region of stability for dipole strength $a_{dd} = 0$ and $= 15a_0$ is shown in figure 3 for (a) 170 and (b) 500 ^{52}Cr atoms as a phase plot of a/a_0 versus the relative strengths of the bichromatic OL ν_ρ and ν_z in radial and axial directions. The stability of a DBEC in a harmonic trap has also been studied [14]. For a fixed a_{dd} and N the stability region lies between the two corresponding lines in figure 3. Above the upper line the system becomes too repulsive (positive Na/a_0) to be confined by the weak bichromatic OL. Below the lower line the system becomes too attractive (negative Na/a_0) and suffers from collapse instability. The localization of a BEC (without dipolar interaction) is controlled by the non-linearity $4\pi aN$ alone of (1) and the effect of the dipolar interaction on the stability of the DBEC is clearly exhibited in figures 3. In these figures we also plot numerical results for collapse instability with negative (attractive) scattering length (the lower limit of stability in this figure), which agree well with the variational results. Starting from a stable localized state, the stability lines (points) are obtained by slowly changing the scattering length

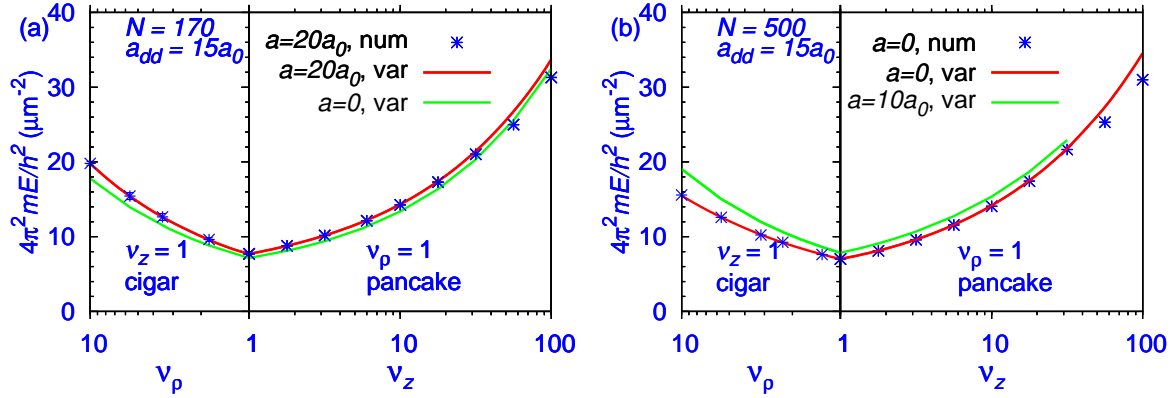


Figure 4. (Color online) Numerical (num) and variational (var) energy E versus relative strengths of bichromatic OL ν_ρ and ν_z for (a) 170 and (b) 500 ^{52}Cr atoms.

a at a fixed trap symmetry (by fixing the parameters ν_ρ and ν_z) until no localized state can be obtained (by numerical or variational means). In the pancake side the dipolar interaction is repulsive and the localization is destroyed for a smaller value of the repulsive scattering length compared to the case where dipolar interaction is absent, as can be seen in figure 3. The opposite happens in the cigar side where the dipolar interaction is attractive. In the cigar side the dipolar interaction is attractive and the localization is destroyed for a larger value of the repulsive scattering length compared to the case where dipolar interaction is absent, as can be seen in figure 3 (b) for 500 atoms. This effect is smaller in figure 3 (a) for 170 atoms.

From (7) we find that $f(\kappa)$ is positive for cigar shape leading to an attractive contribution to energy (6), whereas it is negative in the pancake shape leading to a repulsive term in energy. For $N = 170$ there is a symmetric state with $w_z = w_\rho$ and $f(\kappa) = 0$ near $\nu_\rho = 1, \nu_z \approx 1.3$ where the dipolar interaction does not contribute and where the DBEC is most stable at the maxima in figure 3 (b). At this point the DBEC acts like a “normal BEC” and the Na/a_0 value at the maximum is independent of N . In the pancake shape, the localization of the DBEC can be easily destroyed due to a large repulsive dipolar interaction in the weak bichromatic OL. In the cigar shape, the large attractive dipolar interaction may lead to the collapse of the localized DBEC more easily than in the absence of dipolar interaction. These aspects are clearly illustrated in figure 3 (b). For $N = 500$ the interactions are stronger than for $N = 170$ and the domain of allowed localization in terms of number of atoms has reduced.

In figures 4 (a) and (b) we compare the numerical and variational energies of the ^{52}Cr DBEC of 170 atoms with $a = 0$ and $20a_0$ and of 500 atoms with $a = 0$ and $10a_0$, respectively. A smaller value of a is required for the stability of 500 atoms [see figure 3 (b)]. The agreement between variational and numerical results is good in general except for $\nu_z \rightarrow 100, \nu_\rho = 1$. In this limit the localized DBEC occupies two sites of the bichromatic OL and does not have a Gaussian shape. This justifies a small disagreement

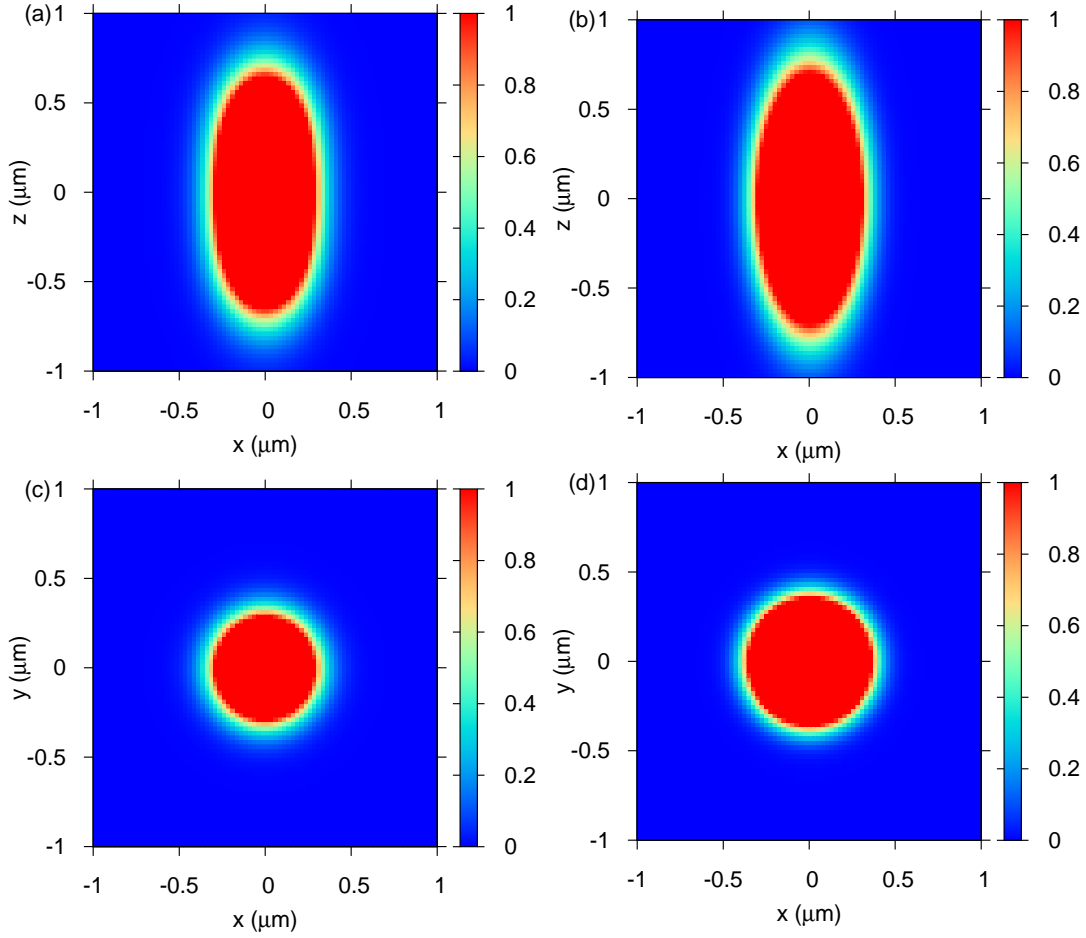


Figure 5. (Color online) 2D Contour plot of density $\phi^2(x, 0, z)$ in the $y = 0$ plane for the cigar-shaped DBEC with $\nu_\rho = 10, \nu_z = 1$ of $N = 500$ ^{52}Cr atoms with $a = 0$: (a) Numerical (b) variational. 2D Contour plot of density $\phi^2(x, y, 0)$ in the $z = 0$ plane for the same DBEC: (c) Numerical (d) variational.

between the numerical and variational results in this limit. The variational result for $a = 10a_0$ in figure 4 (b) only exists up to $\nu_z \approx 35$ [see figure 3 (b)].

Next we study how the DBEC solely under the effect of dipolar interaction ($a = 0$) changes its shape as we move from the cigar to pancake shaped configuration. In figures 5 (a) and (b) we show the 2D contour plot from the numerical and variational analysis, respectively, for density $\phi^2(x, 0, z)$ in the $y = 0$ plane for a cigar-shaped DBEC with $\nu_\rho = 10, \nu_z = 1$ for 500 ^{52}Cr atoms for $a = 0$. The 2D contour plot from the numerical and variational analysis, respectively, for density $\phi^2(x, y, 0)$ in the $z = 0$ plane for the same DBEC is shown in figures 5 (c) and (d), respectively. This localized numerical DBEC state is of small size, compared to its variational counterpart, due to the attractive dipolar interaction in the cigar-shaped DBEC. The attraction due to dipolar interaction has caused the DBEC to contract from an average Gaussian shape. The corresponding numerical and variational energies of the localized states of figures 5 are 15.16 and 15.53, respectively. The localized DBEC states in figures 5 (and also in

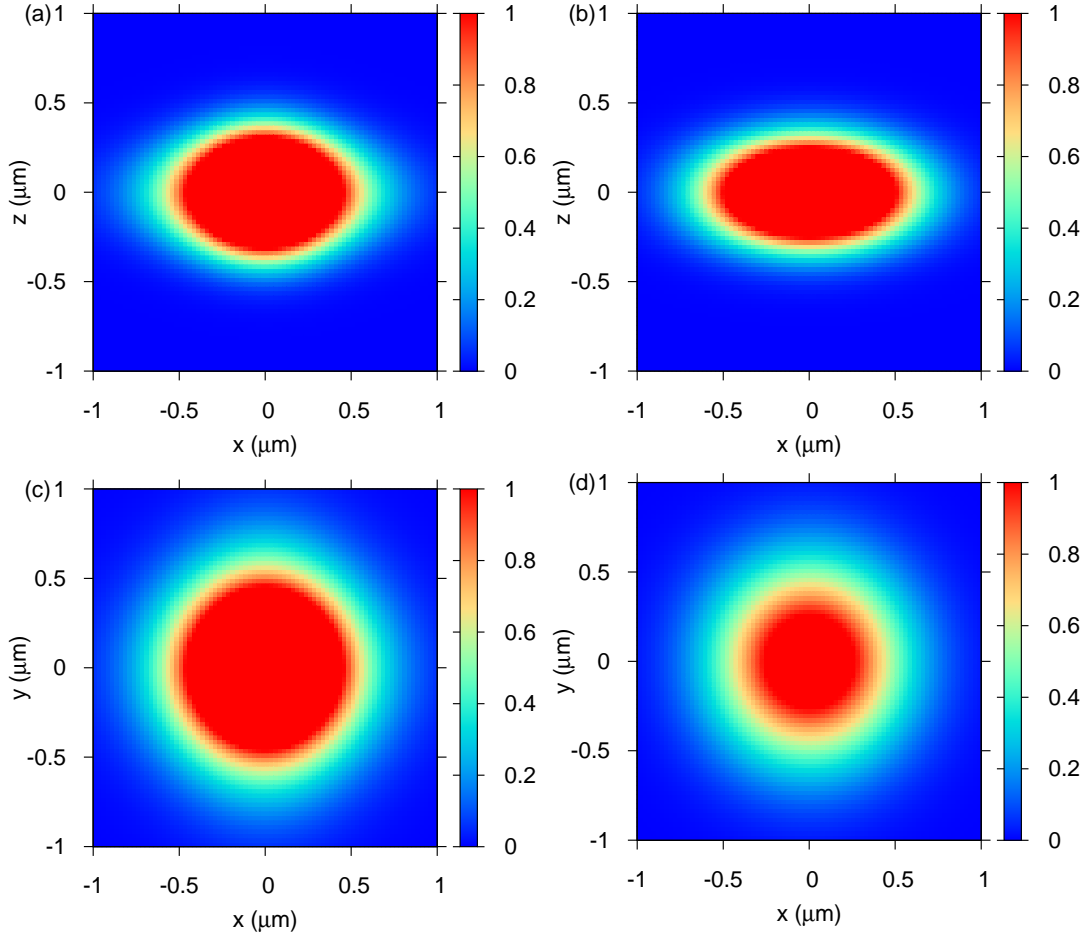


Figure 6. (Color online) Same as in figure 5 for the DBEC in the pancake trap with $\nu_\rho = 1, \nu_z = 10$.

figures 6) occupy practically a single bichromatic OL site at the origin along x, y and z : $-1.25 \mu\text{m} < x, y, z < 1.25 \mu\text{m}$. However, these localized states have exponential tails.

The effect of the dipolar interaction is small in the symmetric case with $\nu_z = \nu_\rho = 1$ and $N = 500$. Nevertheless, due to the complicated dipolar interaction, the density $\phi^2(x, 0, z)$ does not have a pure circular shape in this case (not explicitly shown). This density distribution will be circular for a BEC without dipolar interaction. (A nearly circular shape for this density is obtained for a DBEC with $\nu_\rho = 1$ and $\nu_z = 1.6$.) The numerical and variational energies for this state are 6.97 and 7.06, respectively.

We next consider the localization for $\nu_z = 10, \nu_\rho = 1$ and $a = 0$. In this pancake shape, the dipolar interaction is repulsive and for 500 ^{52}Cr atoms a localized DBEC is obtained. In figures 6 (a) and (b) we show the numerical and variational 2D contour plots of density $\phi^2(x, 0, z)$ in the $y = 0$ plane, respectively, for this DBEC. The numerical and variational 2D contour plots for density $\phi^2(x, y, 0)$ in the $z = 0$ plane for the same DBEC is shown in figures 6 (c) and (d), respectively. In this case, the dipolar interaction is repulsive in nature and hence the size of the DBEC is larger than the

Gaussian variational shape (see figures 5 where the opposite happens for a DBEC with attractive dipolar interaction.). The numerical and variational energies for this state are 14.16 and 14.26, respectively. The change from a cigar shape to a pancake shape of the localized DBEC as we move from $\nu_\rho = 10$ and $\nu_z = 1$ to $\nu_\rho = 1$ and $\nu_z = 10$ is obvious from the density distribution in figures 5 (a) and 6 (a). Although the variational and numerical energies (studied in figures 5 and 6) are quite close to each other, the numerically obtained matter density should have some peculiarities not obtainable from the variational calculation due to the anisotropic dipolar interaction. (The variational calculation is based on an axially-symmetric Gaussian distribution.)

4. Summary and Conclusion

We investigated the localization of a ^{52}Cr DBEC with in a weak bichromatic OL trap in the presence and absence of short-range interaction using the numerical and variational solution of the 3D GP equation (1). Of the two solutions, the numerical solution is the most precise one and should be used in case of disagreement with the variational solution. Although the density of the central part of the localized states has a near Gaussian distribution, the density distribution also has a long exponential tail [3, 4]. The Gaussian distribution near the center permits a variational analysis of localization, which is used for an analytical understanding of the problem. A DBEC of a small number of atoms with a weak short-range interaction could be localized by a relatively weak bichromatic OL trap. From the variational solution we obtain a phase diagram [figure 3 (b)] illustrating the effect of the dipolar interaction on the localization as a function of the strengths of the trap ν_z and ν_ρ in axial and radial directions, respectively. We find that for ^{52}Cr atoms, the dipolar interaction has a moderate effect on localization. (Larger effect will certainly appear for dipolar molecules where the dipole moment could be larger by an order of magnitude compared to the dipole moment of ^{52}Cr atoms.) The numerical and variational energies of the DBEC, as well as the corresponding densities are in reasonable agreement with each other. In the absence of a short-range interaction, the localized DBEC can accommodate the largest number of ^{52}Cr atoms (~ 1000) in the spherical configuration and this number reduces both for cigar and pancake shapes due to the attractive and repulsive dipolar interaction, respectively. The attractive dipolar interaction leads to collapse and the repulsive dipolar interaction leads to leakage to infinity. We hope that this study will motivate experiments on the localization of a ^{52}Cr DBEC in a bichromatic OL trap. The estimate of the number of localized ^{52}Cr atoms, their radial and axial sizes and shapes etc. as predicted in the present study can be verified in the experiment.

Acknowledgments

FAPESP and CNPq (Brazil) and DST (India) provided partial support.

References

- [1] Anderson P W 1958 *Phys. Rev.* **109** 1492
- [2] Chabé J *et al.* 2008 *Phys. Rev. Lett.* **101** 255702
 Edwards E E *et al.* 2008 *Phys. Rev. Lett.* **101** 260402
- [3] Billy J *et al.* 2008 *Nature* **453** 891
- [4] Roati G *et al.* 2008 *Nature* **453** 895
- [5] Inouye S *et al.* 1998 *Nature* 1998 **392** 151
- [6] Aubry S and André G 1980 *Ann. Israel Phys. Soc.* **3** 133
 Kopidakis G, Komineas S, Flach S and Aubry S 2008 *Phys. Rev. Lett.* **100** 084103
- [7] Albert M and Leboeuf P 2010 *Phys. Rev. A* **81** 013614
- [8] Boers D J, Goedeke B, Hinrichs D and Holthaus M 2007 *Phys. Rev. A* **75** 063404
 Sanchez-Palencia L *et al.* 2007 *Phys. Rev. Lett.* **98** 210401
 Clément D *et al.* 2005 *Phys. Rev. Lett.* **95** 170409
 Lye J E *et al.* 2005 *Phys. Rev. Lett.* **95** 070401
 Damski B *et al.* 2003 *Phys. Rev. Lett.* **91** 080403
 Schulte T *et al.* 2005 *Phys. Rev. Lett.* **95** 170411
 Roux G *et al.*, 2008 *Phys. Rev. A* **78** 023628
 Roscilde T 2008 *Phys. Rev. A* **77** 063605
 Paul T *et al.* *Phys. Rev. A* **80** 033615
- [9] Modugno M 2009 *New. J. Phys.* **11** 033023
 Larcher M, Dalfovo F and Modugno M 2009 *Phys. Rev. A* **80** 053606
- [10] Cheng Y and Adhikari S K 2010 *Phys. Rev. A* **82** 013631
 Adhikari S K and Salasnich L 2009 *Phys. Rev. A* **80** 023606
- [11] Cheng Y and Adhikari S K 2010 *Phys. Rev. A* **81** 023620
- [12] Adhikari S K 2010 *Phys. Rev. A* **81** 043636
- [13] Lahaye T *et al.* 2007 *Nature* **448** 672
 Lahaye T *et al.* 2009 *Rep. Prog. Phys.* **72** 126401
 Koch T *et al.* 2008 *Nature Phys.* **4** 218
 Stuhler J *et al.* 2005 *Phys. Rev. Lett.* **95** 150406
 Griesmaier A *et al.* 2005 *Phys. Rev. Lett.* **94** 160401
- [14] Góral K and Santos L 2002 *Phys. Rev. A* **66** 023613
 Yi S and You L 2001 *Phys. Rev. A* **63** 053607
- [15] Dutta O and Meystre P 2007 *Phys. Rev. A* **75** 053604
- [16] Parker N G, Ticknor C, Martin A M and O'Dell D H J 2009 *Phys. Rev. A* **79** 013617
 Ticknor C, Parker N G, Melatos A, Cornish S L, O'Dell D H J and Martin A M 2008 *Phys. Rev. A* **78** 061607
- [17] Santos L, Shlyapnikov G V and Lewenstein M 2003 *Phys. Rev. Lett.* **90** 250403
 Yi S, You L and Pu H 2004 *Phys. Rev. Lett.* **93** 040403
 Góral K, Santos L and Lewenstein M 2002 *Phys. Rev. Lett.* **88** 170406
 Giovanazzi S, O'Dell D and Kurizki G 2002 *Phys. Rev. Lett.* **88** 130402
- [18] Metz J *et al.* 2009 *New J. Phys.* **11** 055032
- [19] Sun B and Pindzola M S 2009 *J. Phys. B* **42** 175301
 Lahaye T *et al.* 2008 *Phys. Rev. Lett.* **101** 080401
- [20] Ronen S, Bortolotti D C E and Bohn J L 2006 *Phys. Rev. A* **74** 013623
- [21] Yi S and You L 2000 *Phys. Rev. A* **61** 041604
- [22] Yi S and You L 2003 *Phys. Rev. A* **67** 045601
- [23] Santos L, Shlyapnikov G V, Zoller P and Lewenstein M 2000 *Phys. Rev. Lett.* **85** 1791
- [24] Wilson R M, Ronen S, Bohn J L and Pu H 2008 *Phys. Rev. Lett.* **100** 245302
- [25] Ronen S, Bortolotti D C E and Bohn J L 2007 *Phys. Rev. Lett.* **98** 030406
- [26] Wilson R M, Ronen S and Bohn J L 2009 *Phys. Rev. A* **80** 023614

- [27] Kuhn R C *et al.* 2005 *Phys. Rev. Lett.* **95** 250403
Skipetrov S E *et al.* 2008 *Phys. Rev. Lett.* **100** 165301
- [28] Pikovsky A S and Shepelyansky D L 2008 *Phys. Rev. Lett.* **100** 094101
Flach S, Krimer D O and Skokos Ch 2009 *Phys. Rev. Lett.* **102** 024101
- [29] Yi S and You L 2004 *Phys. Rev. Lett.* **92** 193201
- [30] Adhikari S K and Muruganandam P 2003 *J. Phys. B: At. Mol. Opt. Phys.* **36** 409
Muruganandam P and Adhikari S K 2003 *J. Phys. B: At. Mol. Opt. Phys.* **36** 2501
- [31] Muruganandam P and Adhikari S K 2009 *Comput. Phys. Commun.* **180** 1888
- [32] Smerzi A, Fantoni S, Giovanazzi S and Shenoy S R 1997 *Phys. Rev. Lett.* **79** 4950
Raghavan S, Smerzi A, Fantoni S and Shenoy S R 1999 *Phys. Rev. A* **59** 620
Albiez M, Gati R, Fölling J, Hunsmann S, Cristiani M and Oberthaler M K 2005 *Phys. Rev. Lett.* **95** 010402
Gati R and Oberthaler M K 2007 *J. Phys. B* **40** R61
Adhikari S K, Lu H and Pu H 2009 *Phys. Rev. A* **80** 063607